Tissue distribution of basigin and monocarboxylate transporter 1 in the adult male mouse: A study using the wild-type and basigin gene knockout mice

3 **AUTHORS**, INCLUDING:

Romana A Nowak
University of Illinois, Urbana-Champaign
87 PUBLICATIONS **1,843** CITATIONS

Tissue Distribution of Basigin and Monocarboxylate Transporter 1 in the Adult Male Mouse: A Study Using the Wild-Type and Basigin Gene Knockout Mice

MASAAKI NAKAI, LI CHEN, AND ROMANA A. NOWAK*

Department of Animal Sciences, University of Illinois, Urbana, Illinois

ABSTRACT

Basigin (Bsg) is a transmembrane protein that is responsible for targeting of monocarboxylate transporters (MCTs) to the cell membrane. The present study was conducted to determine whether or not Bsg was required for the proper localization of MCT isoform 1 (MCT1) in a wide range of tissues in adult male mice. The tissue distributions of Bsg and MCT1 in wild-type (WT) mice, the tissue distribution of MCT1 in Bsg gene knockout (Bsg-KO) mice, and the protein and mRNA levels of MCT1 in both genotypes were studied. Immunohistochemistry demonstrated that Bsg colocalized with MCT1 in the cerebrum, retina, skeletal and cardiac muscle, duodenal epithelium, hepatic sinusoid, proximal uriniferous tubules, Leydig cells, and efferent ductule epithelium in WT mice. Bsg was absent but MCT1 was present in Sertoli cells, cauda epididymis, myoepithelial cells and duct of the mandibular gland, surface epithelium of the stomach and bronchioles. In Bsg-KO mice, with the exception of Leydig cells, MCT1 immunostaining was greatly reduced in intensity and its distribution was altered in tissues that expressed both Bsg and MCT1 in WT mice. Levels of the protein and mRNA for MCT1 in these tissues did not change significantly in Bsg-KO mice. On the other hand, immunostaining patterns in cells in which Bsg was absent but MCT1 was present in WT mice remained unchanged in Bsg-KO mice. These observations suggest that Bsg is required for the proper localization of MCT1 in a wide range of cells but not in every cell type. Anat Rec Part A 288A:527–535, 2006.   © 2006 Wiley-Liss, Inc.

Key words: basigin; monocarboxylate transporter 1; mouse; gene knockout; immunohistochemistry; Western blotting; real time polymerase chain reaction

Basigin (Bsg), also known as CD147, extracellular matrix metalloproteinase inducer (EMMPRIN), neurothelin, 5A11, gp42, OX-47, and CE9, is a highly glycosylated transmembrane protein distributed widely in various organs (Muramatsu and Miyauchi, 2003; Kadomatsu and Muramatsu, 2004). Basigin is involved in a number of physiological and pathological events, including spermatogenesis (Igakura et al., 1998; Maekawa et al., 1998; Toyama et al., 1999; Yuasa et al, 2001; Chen et al., 2004), sperm-egg interaction (Saxena et al., 2002), embryo implantation (Igakura et al., 1998), neural functions such as vision, behavior, memory, and olfaction (Naruhashi et al., 1997; Fan et al., 1998; Hori et al., 2000; Ochrietor et al.,

2001; Philp et al., 2003a, 2003b), immune responses (Pushkarsky et al., 2001), injury repair (Betsuyaku et al.,

*Correspondence to: Romana A. Nowak, Department of Animal Sciences, Room 310, University of Illinois, 1207 W. Gregory Drive, Urbana, IL 61801. Fax: 217-333-8286.
E-mail: ranowak@uiuc.edu

2003), and tumor invasion (Biswas et al., 1995; Zucker et al., 2001), though its mode of action has not been fully elucidated. One of Bsg's proposed functions is that it serves as a chaperone protein to target monocarboxylate transporters (MCTs) to the cell surface (Kirk et al., 2000).

Monocarboxylate transporters are widely expressed on the cell surface and are responsible for the efflux and influx of monocarboxylates such as lactate across the plasma membrane in a variety of organs (Garcia et al., 1994, 1995; Halestrap and Price, 1999; Bonen, 2001). To date, 14 isoforms (MCT1–14) of the MCT family have been described (Halestrap and Price, 1999; Halestrap and Meredith, 2004; Kadomatsu and Muramatsu, 2004). Recent studies have demonstrated that Bsg colocalizes with MCTs in isolated heart cells, cell lines, and epithelial cells of the thyroid and retina (Kirk et al., 2000; Wilson et al., 2002; Fanelli et al., 2003; Philp et al., 2003a). Basigin interacts with MCT1 and MCT4 via its transmembrane and cytoplasmic domains, where Bsg is associated with two MCT1 molecules in the plasma membrane (Kirk et al., 2000; Wilson et al., 2002). Investigators also reported that the expression of MCTs was perturbed when Bsg expression was blocked with an antibody (Kirk et al., 2000). Furthermore, using the Bsg gene knockout (Bsg-KO) mice, it was shown that expression of MCTs was reduced in the retinal epithelium in the absence of Bsg (Philp et al., 2003b). These observations suggest that Bsg is required for the proper expression of MCTs on the cell surface. However, it is not clear whether Bsg is required for proper MCT localization in cells other than isolated cell lines and the retina.

The purpose of the present study was to determine whether or not Bsg is required for the normal localization of MCT1 to the cell surface in a broad range of tissues/cells. First, we studied the tissue distributions of Bsg and MCT1 in the skeletal muscle, cerebrum, eye, testis, epididymis, seminal vesicle, kidney, stomach, duodenum, liver, heart, lung, and salivary glands in the adult wild-type (WT) mice by immunohistochemistry and Western blotting. Second, we determined the distribution of MCT1 in these same tissues in Bsg-KO mice. Finally, tissues that showed changes in MCT1 distribution in Bsg-KO mice were studied by Western blotting and real-time polymerase chain reaction (PCR) in order to determine whether or not the changes in distribution in the absence of Bsg were associated with changes in the levels of MCT1 protein and mRNA.

MATERIALS AND METHODS
Animals

The protocol used in the present study had been approved by the University of Illinois Institutional Animal Care and Use Committee, in accordance with the National Institutes of Health guidelines for the use of animals in research. The wild-type C57BL/6NHsd male mice were obtained from Harlan (Indianapolis, IN). They were housed one per cage with a 12-hr dark/light cycle and allowed free access to water and pelleted food until euthanasia.

Heterozygous (Bsg$^{+/-}$) mice were a kind gift from Dr. Takashi Muramatsu, Department of Biochemistry, Nagoya University School of Medicine, Japan (Igakura et al., 1998). Heterozygote breeding was carried out in the animal facility of the University of Illinois. At 3 weeks of age, the male offspring was anesthetized by isoflurane

inhalation (Attane; Minrad, Bethlehem, PA) and tail snips were collected for genotyping. DNA was extracted from the snips using REDExtract-N-Amp (Sigma, St. Louis, MO), and the genotype was determined by PCR using primers for Bsg and neomycin (Igakura et al., 1998). Offspring with the Bsg gene null mutant ($-/-$) phenotype were maintained under the same conditions as those for the WT mice.

Tissue Collection

The WT (n = 10, 13 weeks of age) and Bsg-KO mice (n = 7, 15–24 weeks of age) were euthanized with carbon dioxide and weighed. Samples of the skeletal muscle (the lateral vastus and rectus femoris), cerebrum, eye (positive control), testis, epididymis, seminal vesicle, kidney, stomach, duodenum, liver, heart, lung, and salivary glands (sublingual and mandibular) were collected immediately. Tissues for histology were fixed in Bouin's solution overnight and processed for paraffin embedding. Tissues for Western blotting analysis were snap-frozen in liquid nitrogen and kept at $-80°C$ until use. Tissues for real-time PCR analysis were placed in RNA later (Sigma) at 4°C overnight and then transferred to $-80°C$.

Western Blotting Analysis

Tissues were ground and proteins were extracted using Laemmli sample buffer. Proteins were separated by sodium dodecyl sulfate polyacrylamide gel electrophoresis and transferred to nitrocellulose membranes. After blocking in 5% nonfat dry milk, the membranes were probed for Bsg with a goat antimouse EMMPRIN (= Bsg) antibody (R&D systems, Minneapolis, MN) at a 1:500 dilution for 1 hr. The lysate of the Bsg-KO mouse lung was used as a negative control to verify the specificity of the antibody. Membranes were then incubated in donkey antigoat immunoglobulin (Ig) G antibody labeled with horseradish peroxidase (HRP; Santa Cruz Biotechnology, Santa Cruz, CA) at a 1:2,500 dilution for 1 hr. The bound secondary antibody was detected using a SuperSignal West Pico substrate kit (Pierce, Rockford, IL).

To compare the MCT1 protein levels between the WT and Bsg-KO mice, proteins of the caput epididymis, kidney, and liver from WT and Bsg-KO mice were prepared for Western blotting analysis. The membranes were incubated with a chicken anti-MCT1 antibody at a 1:500 dilution (Chemicon International, Temecula, CA). Protein lysates of the lung and liver were incubated with preimmune IgY (Chemicon International) as a control. Membranes were then incubated with an HRP-labeled goat antichicken IgG (= IgY) antibody (Kirkegaard and Perry Laboratories, Gaithersburg, MD) at a dilution of 1:15,000. The reaction was detected with the same kit as used for Bsg. After detection of MCT1, the membranes were stripped with Western blotting strip buffer (Pierce) for 20 min. Subsequently, membranes were reprobed for actin as the loading control with a rabbit antiactin antibody at a 1:3,000 dilution (Sigma), followed by a goat antirabbit Ig antibody at a 1:20,000 dilution (BD Transduction Laboratories, Lexington, KY).

Histology and Immunohistochemistry

Paraffin sections were cut serially at 4 μm and stained with hematoxylin and eosin for histological observation. Sections for Bsg immunostaining were boiled in 0.01 M

citrate buffer for 10 min using a microwave oven to unmask the antigen. Sections were immersed in 0.3% H_2O_2 in methanol for 15 min to inactivate endogenous peroxidase, incubated with 5% normal rabbit serum for 10 min to block nonspecific binding of antibodies, then incubated with the same primary antibody as used for the Western blotting at a dilution of 1:100 overnight at 4°C. Tissues of Bsg-KO mice were used as the negative control. Sections were then incubated in biotinylated rabbit antigoat antibody at a 1:100 dilution and the positive reaction was visualized using a Vectastain ABC kit (Vector Laboratories, Burlingame, CA). Immunostaining of MCT1 did not require the antigen retrieval. Sections were treated with 0.3% H_2O_2 in methanol and 5% normal goat serum. Sections were then incubated with a chicken anti-MCT1 antibody at 1:200–400 dilutions overnight at 4°C. Control sections were incubated with the preimmune chicken IgY. The same secondary antibody used for the Western blotting was applied at a dilution of 1:100. The positive reaction was detected using 3,3′-diaminobenzidine and hydrogen peroxide. Nuclei were counterstained with hematoxylin for all sections.

Sections of eyes were immunostained by the indirect immunofluorescence method because the DAB reaction product could not be seen due to the melanin in the retinal pigment epithelium. Primary antibodies for Bsg and MCT1 were used at dilutions of 1:400 and 1:800, respectively. Positive immunostaining was visualized using the fluorescein-5-isothiocyanate-labeled goat antichicken IgY (Kirkegaard and Perry Laboratories) and rabbit antigoat IgG (Sigma) at a 1:100 dilution.

Real-Time Polymerase Chain Reaction

Tissues of the kidney, liver, and the caput epididimis from WT and Bsg-KO mice were homogenized in TRIzol reagent and RNA was extracted according to the manufacturer's instruction (Invitrogen, Carlsbad, CA). After quantification of RNA, complementary DNA (cDNA) was prepared using an iScript cDNA synthesis kit (Bio-Rad Laboratories, Hercules, CA). Then, cDNAs for MCT1 and glyceraldehyede-3-phosphate dehydrogenase (GAPDH, internal control) were quantified in triplicate by real-time PCR using a 7900HT Fast Real-Time PCR System (Applied Biosystems, Foster City, CA). The PCR primers and probes for MCT1 and GAPDH were purchased from Applied Biosystems. No RNA and no template controls were included. The difference in threshold cycles for MCT1 and GAPDH of each organ was compared between the genotypes.

Statistical Analysis

Quantitative data of the real-time PCR were compared between WT and Bsg-KO mice using the Student's t-test. Differences were considered significant when the P value was smaller than 0.05.

RESULTS
Antibody Specificity

Western blotting analysis of lung proteins from the Bsg-KO mouse produced no band (Fig. 1a), which verified the specificity of the antibody to mouse Bsg. Incubation of the proteins from the lung and liver of the WT mouse with the anti-MCT1 antibody produced a band around 43 kDa. This band was not seen when the membrane had been
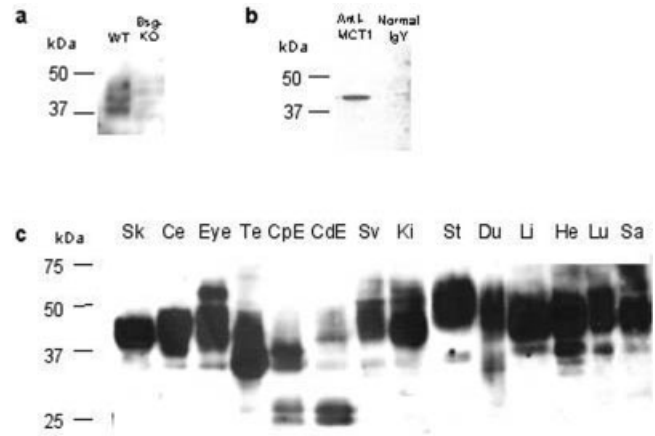

Fig. 1. Western blotting analyses for Bsg and MCT1 proteins. **a:** Lung proteins of the WT and Bsg-KO mice probed for Bsg. A broadband characteristic of Bsg is seen in the WT but no band is seen in the Bsg-KO, confirming the specificity of the antibody. **b:** Lung proteins of the WT mouse probed with an anti-MCT1 antibody and preimmune normal chicken IgY. The antibody produces a band at 43 kDa, which is not seen when probed with normal IgY. **c:** Basigin is present in all organs studied in the WT. The molecular weight (MW) ranges from approximately 26 to 65 kDa, with the largest MW in the eye, kidney (Ki), and stomach (St) and the lowest MW in the caput epididimis (CpE) and cauda epididimis (CdE). Sk, skeletal muscle; Ce, cerebrum; Te, testis; Sv, seminal vesicle; Du, duodenum; Li, liver; He, heart; Lu, lung; Sa, salivary gland (mandibular and sublingual glands).

incubated with the preimmune chicken IgY (Fig. 1b), confirming the specificity of the antibody to MCT1.

Western Blotting Analysis of Bsg in WT Mice

The anti-Bsg antibody produced a characteristic broad range of protein bands in the various organs studied in WT mice (Fig. 1c). The molecular weight of Bsg ranged from 25 to 60 kDa, with the highest molecular weight observed in the eye, kidney, and stomach and the lowest molecular weight in the epididimis. The various molecular weights for Bsg are due to varying degrees of glycosylation, which appear to be tissue-dependent (Fig. 1c).

Histology and Immunohistochemistry of Bsg and MCT1 in WT Mice

No histological abnormalities were observed in any organs in WT mice. Histological sections from Bsg-KO mice stained for Bsg produced no positive immunoreactivity. Based on the immunostaining pattern of MCT1 with or without a colocalization of Bsg, tissues/cells were classified into two groups: group 1, in which both Bsg and MCT1 were present (Table 1), and group 2, in which Bsg was absent but MCT1 was present (Table 2).

In group 1, the capillary endothelium in the cerebrum was strongly positive for Bsg and MCT1. The ependyma cells showed positive immunoreactivity for both Bsg and MCT1 in the apical cytoplasm. The epithelial cells of the choroid plexus were consistently positive for Bsg but not always positive for MCT1. In the eye, positive immunoreactivity for Bsg was observed on the apical and basolateral surfaces of the retinal pigment epithelial cells and the stratum neuroepitheliale (outer plexiform layer, inner nu-

TABLE 1. Tissues/cells that express both Bsg and MCT1 proteins (Group 1)

Organ	Tissue/Cell	Bsg/WT	MCT1/WT	MCT1/Bsg-KO
Cerebrum	Capillary endothelium	+	+	−
	Ependyma	+	+	+
	Choroid Plexus epithelium	+	+,−	+,−
Eye	Pigment epithelium	+	+	−
	Stratum neuroepiteliale	+	+	−
	Capillary endothelium	+	+	−
Skeletal muscle	Skeletal muscle fiber	+	+	−*
Heart	Cardiac muscle fiber	+	+	−*
Duodenum	Surface epithelium	+	+	−
Liver	Sinusoid endothelium	+	+	−
Kidney	Proximal tubule epithelium	+	+	−
Testis	Leydig cell	+	+	+
Epididymis	Efferent ductule epithelium	+	+	−*

* MCT1 is decreased in staining intensity and alters in distribution.

TABLE 2. Tissues/cells that express MCT1 but not Bsg proteins (Group 2)

Organ	Tissue/Cell	Bsg/WT	MCT1/WT	MCT1/Bsg-KO
Testis	Sertoli cell	−	+,−	+,−
Epididymis	Cauda epithelium	−	+	+
Seminal vesicle	Smooth muscle	−	+	+
Mandibular	Myoepithelial cell	−	+	+
	Ductal epithelium	−	+	+
Stomach	Surface epithelium	−	+	+
Lung	Bronchiole epithelium	−, ±	+	+

clear layer, and the inner half of the layer of rods and cones). Monocarboxylate transporter 1 showed a similar staining pattern to that of Bsg except that it was negative on the basolateral surface of the retinal pigment epithelial cells. The capillary endothelium in the retina was also strongly positive for Bsg and MCT1. Skeletal muscle fibers, but not all, showed Bsg expression mainly on the cell surface (Fig. 2a), while MCT1 was present both on the cell surface and in the cytoplasm (Fig. 2b). Cardiac muscle fibers were positive for both Bsg (Fig. 2c) and MCT1 (Fig. 2d) on the cell surface, in particular at the intercalated disks. In the duodenum, Bsg and MCT1 were present on the basolateral aspect of the surface epithelium of the villi and smooth muscle fibers of the tunica muscularis. Basigin (Fig. 2e) and MCT1 (Fig. 2f) immunoreactivities in the liver were found exclusively along the sinusoidal wall. In the kidney, intense immunoreactivity for Bsg (Fig. 2g) and MCT1 (Fig. 2h) was seen in the basal cytoplasm of epithelial cells lining the initial part of the proximal convoluted tubules. In the testis, both Bsg (Fig. 2i) and MCT1 (Fig. 2j) were intensely positive in Leydig cells, where Bsg was present on the cell surface and MCT1 was present throughout the cytoplasm. In the caput epididymis, ciliated cells of the efferent ductules were strongly positive for both Bsg (Fig. 2k) and MCT1 (Fig. 2l).

In group 2, Sertoli cells in the testis occasionally showed some weak immunostaining for MCT1. There was no Bsg immunoreactivity throughout the epididymis except for sperm tails (Fig. 3a). MCT1 was negative in the caput but became positive caudally along the luminal border of the epithelium in the corpus and cauda epididymis (Fig. 3b). In the seminal vesicle, subepithelial smooth muscle fibers were strongly positive for MCT1. The mandibular gland showed no Bsg immunoreactivity (Fig. 3c) but intense staining for MCT1 in myoepithelial cells surrounding the glandular portion and the ductal epithelium (Fig. 3d). In the stomach, superficial epithelial cells were negative for Bsg (Fig. 3e) but strongly positive for MCT1 (Fig. 3f). In the lung, MCT1 immunoreactivity was observed in the cytoplasm of the bronchiole epithelial cells as well as in the subepithelial smooth muscle fibers of the bronchioles.

Histology and Immunohistochemistry of MCT1 in Bsg-KO Mice

Although Bsg is widely distributed in WT mice, Bsg-KO mice showed histological abnormalities only in the testis and retina as reported elsewhere. Briefly, there were only a few young round spermatids and no sperm in the testis. The Leydig cells appeared normal. In the retina, the layer of rods and cones, external nuclear layer and external plexiform layer were thinner in Bsg-KO mice than in WT mice.

The lack of Bsg resulted in a significant change in MCT1 immunostaining in tissues/cells of group 1 (Fig. 4, Table 1). In the skeletal muscle, MCT1 immunoreactivity of the cell surface almost disappeared and accumulated densely in the perinuclear area that was located immediately under the cell surface (Fig. 4a). In cardiac muscle fibers, MCT1 immunostaining shifted from the cell surface and intercalated disks to the perinuclear area and formed fine granules (Fig. 4b). Monocarboxylate transporter 1 immunoreactivity disappeared from the retina, liver (Fig. 4c), kidney (Fig. 4d), duodenum, and capillary endothelium of the cerebrum in the Bsg-KO mouse. In the testis, the presence of MCT1 was not confirmed in the sperm tail because sperm were not formed. In the efferent ductules, MCT1 expression disappeared from the basolateral surface and instead there was a weak immunoreactivity on the luminal border of the ciliated epithelial cells (Fig. 4f). In group 2 of Bsg-KO mice, localization of MCT1 did not
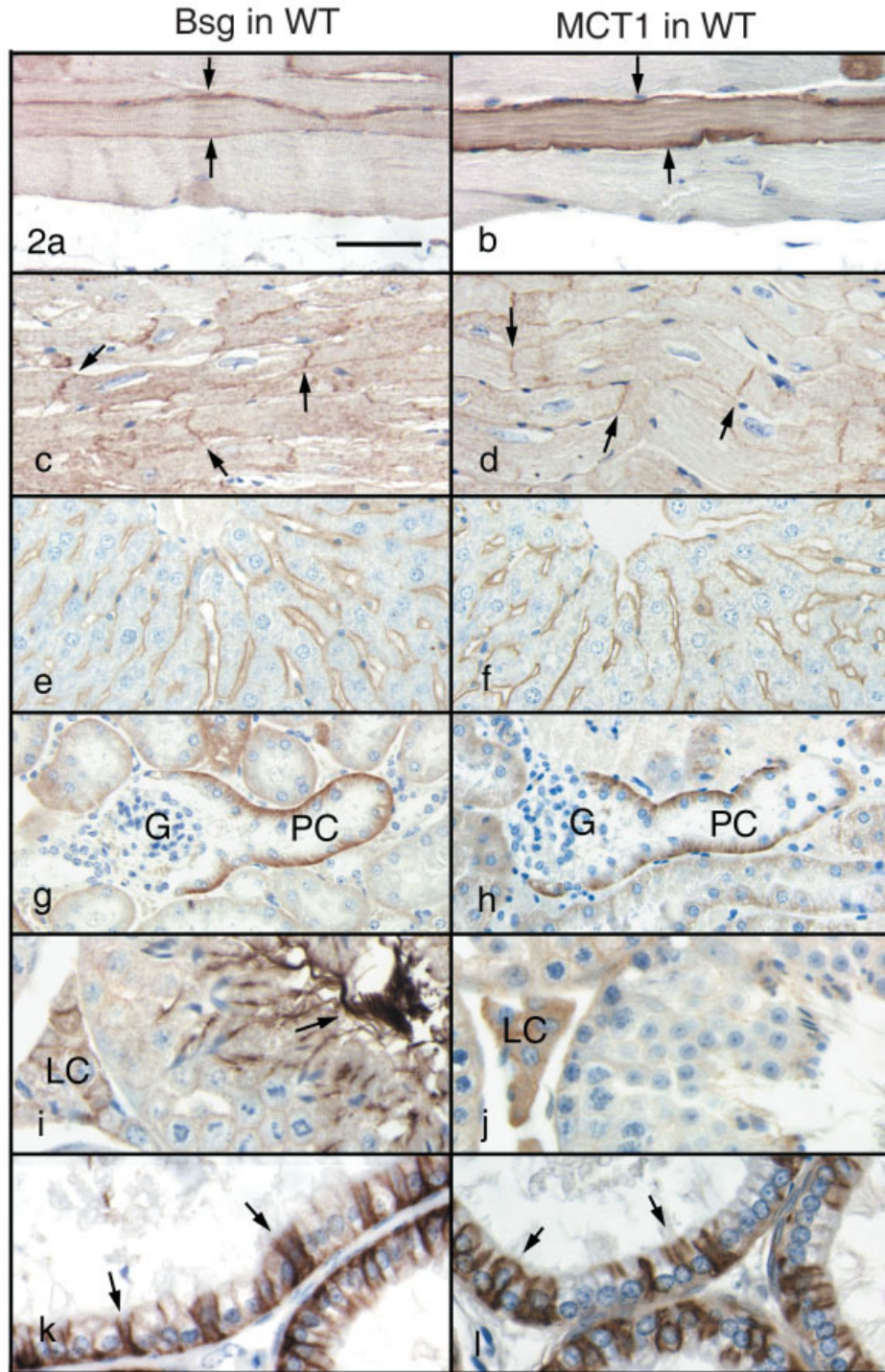
Fig. 2. Immunohistochemistry for Bsg (left column) and MCT1 (right column) in group 1 of the WT mice. Scale bar = 50 μm. In skeletal muscle fibers, Bsg is seen on the cell surface (**a**, arrows) and MCT1 is in the cytoplasm and on the cell surface (**b**, arrows). In cardiac muscle fibers, Bsg (**c**) and MCT1 (**d**) are seen on the cell surface, especially at the intercalated disks (arrows). In the liver, Bsg (**e**) and MCT1 (**f**) are seen along the sinusoidal wall. In the kidney, Bsg (**g**) and MCT1 (**h**) are seen in the basal cytoplasm of epithelial cells lining the initial part of the proximal convoluted tubule (PC). G, glomerulus. In the testis, Bsg (**i**) is present in the sperm tail (arrow) and on the Leydig cell (LC) surface. MCT1 (**j**) is seen in Leydig cells (LC). In the efferent ductules, intense Bsg (**k**) and MCT1 (**l**) immunoreactions are seen on the basolateral surface of ciliated cells (arrows).
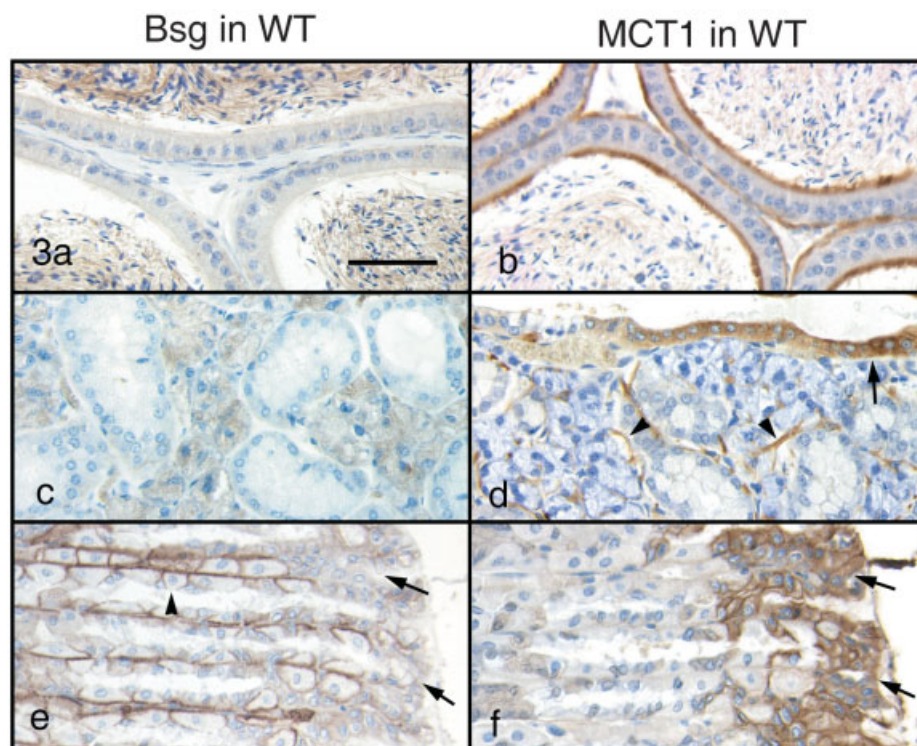
Fig. 3. Immunohistochemistry for Bsg (left column) and MCT1 (right column) in group 2 of the WT mice. Scale bar = 50 μm. In the cauda epididymis, Bsg (**a**) is negative except for sperm tails but MCT1 is strongly positive along the brush border of the epithelium (**b**). In the mandibular gland, Bsg (**c**) is absent but MCT1 (**d**) is present on the duct epithelium (arrow) and myoepithelial cells (arrowheads). In the stomach, Bsg is absent (**e**, arrows) but MCT1 is present in gastric superficial cells (**f**, arrows). Note that parietal cells (arrowhead) are positive for Bsg on the basolateral surface but negative for MCT1.

differ significantly from that of WT mice in all cell types (Fig. 5, Table 2).

Western Blotting and Real-Time PCR Analyses of MCT1 in WT and Bsg-KO Mice

Since there was a great reduction in MCT1 immunostaining in group 1 of the Bsg-KO mice as shown in Figure 2, we studied MCT1 protein levels in the liver, kidney, and caput epididymis in both genotypes by immunoblotting. However, there were no significant differences in MCT1 protein levels in any of these tissues between the two genotypes (Fig. 6).

Differences in MCT1 mRNA levels were assessed by real-time PCR. The differences in threshold cycle for MCT1 in the kidney, liver, and caput epididymis of Bsg-KO mice did not differ from those of the WT (Table 3), indicating that no change in mRNA levels for MCT1 was induced in the Bsg-KO mice.

DISCUSSION

The purpose of the present study was to determine whether or not Bsg was required for the proper localization of MCT1 in various organs. In order to answer this question, we analyzed tissue distributions of Bsg and MCT1 proteins in WT mice; differences in tissue distribution of MCT1 in the Bsg-KO mice compared with WT mice; and differences in mRNA and protein levels of MCT1 in the Bsg-KO mice compared to WT mice. Our results showed that Bsg and MCT1 proteins colocalized in a wide range of tissues, including the cerebrum, eye, skeletal muscle, heart, duodenum, liver, kidney, testis, and efferent ductule in the WT mouse. Examination of the Bsg-KO mouse showed that the lack of Bsg resulted in a disappearance or great reduction in MCT1 immunostaining in these organs except for the Leydig cells in the testis. In addition, abnormal distribution of MCT1 was observed in cardiac muscle, skeletal muscle, and efferent ductule epithelium. In contrast, there were cells that expressed only MCT1 in the testis, epididymis, seminal vesicle, mandibular gland, stomach, and lung. These observations indicate that Bsg is required for the proper localization of MCT1 not only in previously reported isolated heart cells, cell lines, and the retina (Kirk et al., 2000; Philp et al., 2003a), but also in many other organs. Our data also suggest that Bsg is not required for MCT1 in every cell type. On the other hand, Western blotting and real-time PCR did not show a significant change in either analysis. Therefore, it is likely that Bsg is not involved in regulation of MCT1 mRNA or MCT1 protein synthesis.

The role of Bsg as a chaperone protein for MCTs was reported in an in vitro study. Basigin was shown to colocalize with MCT1 on the cell surface, especially on the intercalated disks, of isolated heart cells (Kirk et al., 2000). This same study showed that transfection of MCTs alone to COS and HELA cells resulted in an accumulation of MCTs in the perinuclear area, whereas transfection of
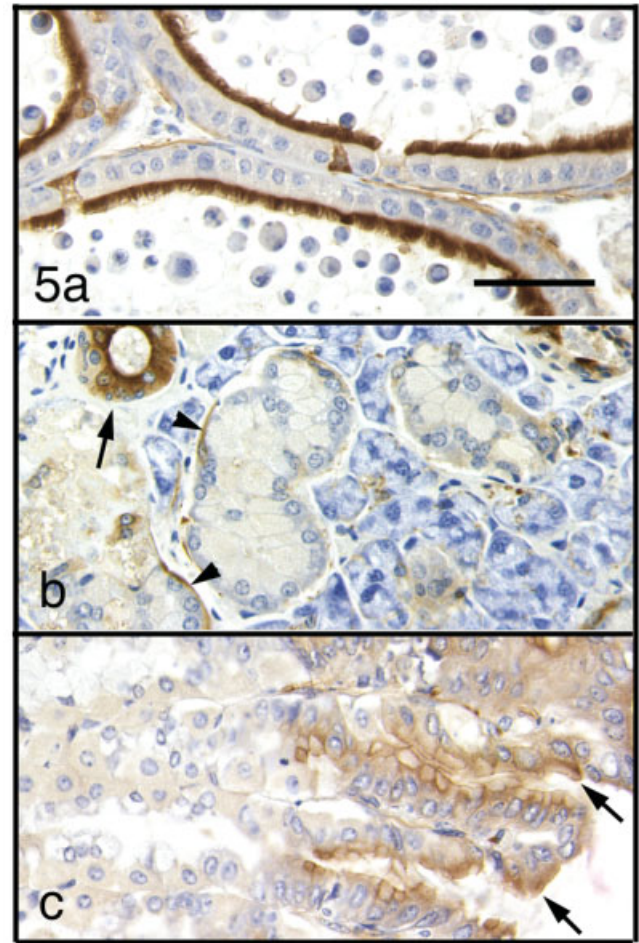
MCT1 in Bsg-KO
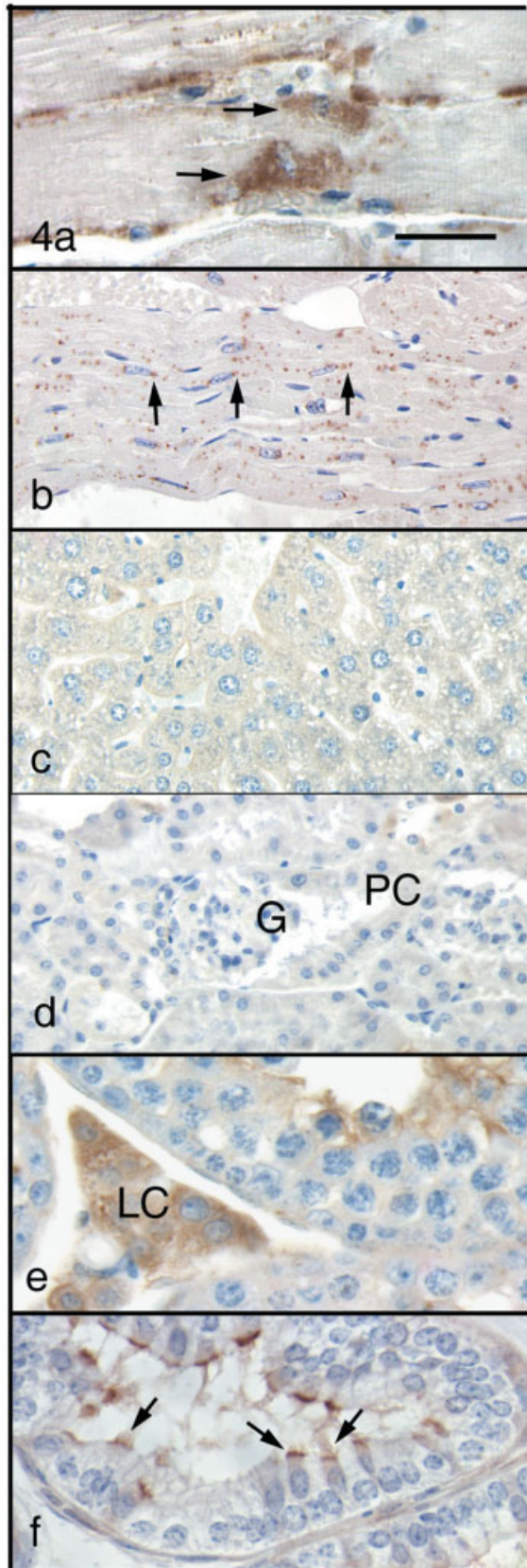
MCT1 in Bsg-KO

Fig. 5. Immunohistochemistry of MCT1 in group 2 of the Bsg-KO mice. Scale bar = 50 μm. Immunostaining patterns of MCT1 in the cauda epididymis (**a**), mandibular gland (**b**), and stomach (**c**) in the Bsg-KO mice do not differ significantly from those in the WT.

MCTs along with Bsg led to the proper targeting of MCTs to the cell surface (Kirk et al., 2000). In the present study, we demonstrated that Bsg and MCT1 colocalized in cardiac and skeletal muscle in WT mice, and that in the absence of Bsg, MCT1 aggregated in the perinuclear area, where cytoplasmic organelles that are involved in protein synthesis such as the Golgi apparatus are present. This change in distribution strongly suggests a failure of MCT1 delivery to the proper position in the cell membrane after

Fig. 4. Immunohistochemistry of MCT1 in group 1 of the Bsg-KO mice. Scale bar = 50 μm. In the skeletal (**a**) and cardiac (**b**) muscles, MCT1 disappears from the cell surface and cytoplasm but accumulates in the perinuclear area (arrows). No MCT1 immunostaining is seen in the liver (**c**) and kidney (**d**). G, glomerulus; PC, proximal convoluted tubule. In the testis, Leydig cells (LC; **e**) remain positive for MCT1 in the absence of Bsg. In the efferent ductules (**f**), MCT1 disappears from the basolateral surface and accumulates on the apical border of ciliated cells (arrows).

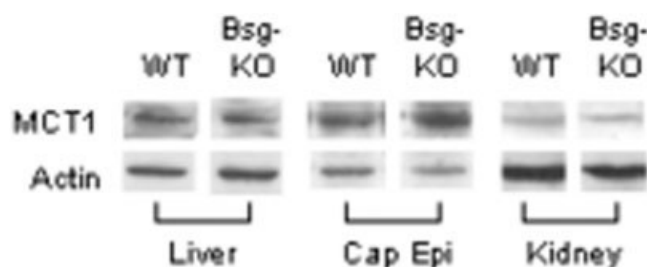534   NAKAI ET AL.

Fig. 6. Western blotting analysis of MCT1 protein levels in the liver, caput epididymis (Cap Epi), and kidney of WT and Bsg-KO mice. There is no significant difference in MCT1 protein level in any organ between the two genotypes. Actin is used as an internal loading control.

TABLE 3. Quantitative analysis of mRNA levels for MCT1 in WT and Bsg-KO mice

Organ	Delta Ct[a] ± SD	
	WT mice	Bsg-KO mice
Liver	6.92 ± 0.37 (n = 4)	7.33 ± 0.87[b] (n = 4)
Kidney	8.37 ± 0.41 (n = 4)	7.45 ± 0.80[b] (n = 4)
Caput epididymis	5.96 ± 0.44 (n = 4)	6.47 ± 0.35[b] (N = 3)

[a]Delta Ct: Difference of cycle threshold between MCT1 and GAPDH.
[b]No significant difference from the WT ($P < 0.05$).

synthesis. Thus, our data are the first to confirm that Bsg is required for the proper localization of MCT1 in cardiac and skeletal muscle in vivo. The functional alterations that would result due to the lack of MCT1 on the cell surface have not been evaluated. However, since efflux and influx of monocarboxylates such as lactate and pyruvate are important in terms of energy supply and intracellular pH regulation (Poole and Halestrap, 1993), cardiac and skeletal muscles of the Bsg-KO mouse could have a functional impairment unless there is some type of compensating mechanism. We also observed a shift in MCT1 immunostaining from the basolateral aspect to the luminal border of the efferent ductule epithelium in Bsg-KO mice, indicating that a failure in proper localization of MCT1 also occurs in this organ. However, the reason for luminal accumulation of MCT1 in this cell type and its significance are not known.

Despite the fact that colocalization of Bsg and MCT1 occurs in an extensive range of tissues/cells in WT mice (group 1), morphological abnormalities in Bsg-KO mice were confined to the retinal epithelium and seminiferous epithelium. These abnormalities were similar to those reported previously (Igakura et al., 1998; Toyama et al., 1999; Hori et al., 2000; Ochrietor et al., 2001; Chen et al., 2004). In addition, tissues/cells of group 2 in WT mice expressed MCT1 alone, and this MCT1 distribution remained unchanged in Bsg-KO mice. Therefore, the present data for group 2 point to the fact that proper MCT1 protein localization does not necessarily depend on the presence of Bsg in every single tissue and cell type. Thus, it is possible that Bsg is not the only molecule that is responsible for the proper expression of MCT1, and that

there is a molecule(s) that can compensate for the lack of Bsg in some cells but not in the retinal and seminiferous epithelia. It was recently reported that embigin, another member of the Ig superfamily, is an ancillary protein for MCT2 (Wilson et al., 2005). However, it is unknown if embigin acts as an ancillary protein for MCT1 when Bsg is absent. In this regard, it would be interesting to study the distribution of embigin in the Bsg-KO mouse. Another implication of the limited phenotypic abnormalities in the Bsg-KO mouse is that there is a mechanism(s), involving other MCT isoforms, that may compensate for the impaired MCT1 expression due to a lack of Bsg. This possibility could also be tested in a future study.

A recent study reported that immunoreactivity for MCT1, MCT3, and MCT4 disappeared from the retina in the Bsg-KO mouse (Philp et al., 2003a). In accordance with this decrease in immunostaining, Western blotting analysis in these animals showed a decrease in MCT1 protein levels as well. This decrease in MCT1 is thought to be due to a rapid metabolism of the protein because it failed to be delivered properly to the cell surface (Kadomatsu and Muramatsu, 2004). We observed in our study that many of the tissues/cells in group 1 either lost or had greatly reduced MCT1 immunostaining in Bsg-KO mice. However, there was no significant difference in protein level by Western blotting or mRNA levels as measured by real-time PCR. The reason for this difference between the immunohistochemistry and immunoblotting and real-time PCR data is not clear. However, one possible explanation would be that MCT1 protein that failed to be targeted properly to the cell membrane might remain diffusely distributed throughout the cytoplasm, where it could be difficult to be visualized microscopically.

When the patterns of localization for Bsg and MCT1 proteins reported in earlier studies were compared to our findings in the present study, differences were noted in several organs. For example, Bsg immunoreactivity was detected in the testis in spermatocytes, spermatids and their flagella, Sertoli cells, and Leydig cells in rodents (Cesario and Bartles, 1994; Cesario et al., 1995; Maekawa et al., 1998). In contrast, Bsg immunoreactivity was only evident in the flagella and on the Leydig cell surface in our study. Monocarboxylate transporter 1 in the testis was localized to different types of germ cells in the rat (Garcia et al., 1994, 1995; Goddard et al., 2003). However, we did not see MCT1 staining in the seminiferous epithelium, except for occasional weak staining in Sertoli cells. We did observe intense staining for MCT1 in Leydig cells. Garcia et al. (1995) saw no MCT1 immunostaining in the kidney and liver, whereas these organs were positive for MCT1 in the present study. However, these investigators did observe immunostaining patterns similar to ours for MCT1 in cardiac muscle. These differences in Bsg and MCT1 immunostaining patterns among various different studies are partly attributable to differences in the antibodies used. Localizations of Bsg and MCT proteins needs to be reconfirmed in these organs.

In conclusion, our study has demonstrated in vivo that Bsg is required for the proper expression of MCT1 protein in a broad range of tissues and cells. In addition, our study is the first to show that there are some cell types that do not require Bsg for the proper MCT1 expression. Since morphological abnormalities are limited in the Bsg-KO mouse, it is likely that there is a molecule(s) that can compensate for the lack of Bsg.

LITERATURE CITED

Betsuyaku T, Kadomatsu K, Griffin GL, Muramatsu T, Senior RM. 2003. Increased basigin in bleomycin-induced lung injury. Am J Respir Cell Mol Biol 28:600–606.

Biswas C, Zhang Y, DeCastro R, Guo H, Nakamura T, Kataoka H, Nabeshima K. 1995. The human tumor cell-derived collagenase stimulatory factor (renamed EMMPRIN) is a member of the immunoglobulin superfamily. Cancer Res 55:434–439.

Bonen A. 2001. The expression of lactate transporters (MCT1 and MCT4) in heart and muscle. Eur J Appl Physiol 86:6–11.

Cesario MM, Bartles JR. 1994. Compartmentalization, processing and redistribution of the plasma membrane protein CE9 on rodent spermatozoa: relationship of the annulus to domain boundaries in the plasma membrane of the tail. J Cell Sci 107:561–570.

Cesario MM, Ensrud K, Hamilton DW, Bartles JR. 1995. Biogenesis of the posterior-tail plasma membrane domain of the mammalian spermatozoon: targeting and lateral redistribution of the posterior-tail domain-specific transmembrane protein CE9 during spermiogenesis. Dev Biol 169:473–486.

Chen S, Kadomatsu K, Kondo M, Toyama Y, Toshimori K, Ueno S, Miyake Y, Muramatsu T. 2004. Effects of flanking genes on the phenotypes of mice deficient in basigin/CD147. Biochem Biophys Res Commun 324:147–153.

Fan QW, Yuasa S, Kuno N, Senda T, Kobayashi M, Muramatsu T, Kadomatsu K. 1998. Expression of basigin, a member of the immunoglobulin superfamily, in the mouse central nervous system. Neurosci Res 30:53–63.

Fanelli A, Grollman EF, Wang D, Philp NJ. 2003. MCT1 and its accessory protein CD147 are differentially regulated by TSH in rat thyroid cells. Am J Physiol Endocrinol Metab 285:E1223–E1229.

Garcia CK, Goldstein JL, Pathak RK, Anderson RG, Brown MS. 1994. Molecular characterization of a membrane transporter for lactate, pyruvate, and other monocarboxylates: implications for the Cori cycle. Cell 76:865–873.

Garcia CK, Brown MS, Pathak RK, Goldstein JL. 1995. cDNA cloning of MCT2, a second monocarboxylate transporter expressed in different cell than MCT1. J Biol Chem 270:1843–1849.

Goddard I, Florin A, Mauduit C, Tabone E, Contard P, Bars R, Chuzel F, Benahmed M. 2003. Alteration of lactate production and transport in the adult rat testis exposed in utero to flutamide. Mol Cell Endocrinol 206:137–146.

Halestrap AP, Price NT. 1999. The proton-linked monocarboxylate transporter (MCT) family: structure, function and regulation. Biochem J 343:281–299.

Halestrap AP, Meredith D. 2004. The SLC16 gene family: from monocarboxylate transporters (MCTs) to aromatic amino acid transporters and beyond. Pflugers Arch 447:619–628.

Hori K, Katayama N, Kachi S, Kondo M, Kadomatsu K, Usukura J, Muramatsu T, Mori S, Miyake Y. 2000. Retinal dysfunction in basigin deficiency. Invest Ophthalmol Vis Sci 41:3128–3133.

Igakura T, Kadomatsu K, Kaname T, Muramatsu H, Fan QW, Miyauchi T, Toyama Y, Kuno N, Yuasa S, Takahashi M, Senda T, Taguchi O, Yamamura K, Arimura K, Muramatsu T. 1998. A null mutation in basigin, an immunoglobulin superfamily member, indicates its important roles in peri-implantation development and spermatogenesis. Dev Biol 194:152–165.

Kadomatsu K, Muramatsu T. 2004 Roles of basigin, a glycoprotein belonging to the immunoglobulin superfamily, in the nervous system. Tapakushitu Kakusan Kouso 49:2417–2424.

Kirk P, Wilson MC, Heddle C, Brown MH, Barclay AN, Halestrap AP. 2000. CD147 is tightly associated with lactate transporters MCT1 and MCT4 and facilitates their cell surface expression. EMBO J 19:3896–3904.

Maekawa M, Suzuki-Toyota F, Toyama Y, Kadomatsu K, Hagihara M, Kuno N, Muramatsu T, Dohmae K, Yuasa S. 1998. Stage-specific localization of basigin, a member of the immunoglobulin superfamily, during mouse spermatogenesis. Arch Histol Cytol 61:405–415.

Muramatsu T, Miyauchi T. 2003. Basigin (CD147): a multifunctional transmembrane protein involved in reproduction, neural function, inflammation and tumor invasion. Histol Histopathol 18:981–987.

Naruhashi K, Kadomatsu K, Igakura T, Fan QW, Kuno N, Muramatsu H, Miyauchi T, Hasegawa T, Itoh A, Muramatsu T, Nabeshima T. 1997. Abnormalities of sensory and memory functions in mice lacking Bsg gene. Biochem Biophys Res Commun 236:733–737.

Ochrietor JD, Moroz TM, Kadomatsu K, Muramatsu T, Linser PJ. 2001. Retinal degeneration following failed photoreceptor maturation in 5A11/Basigin null mice. Exp Eye Res 72:467–477.

Philp NJ, Ochrietor JD, Rudoy C, Muramatsu T, Linser PJ. 2003a. Loss of MCT1, MCT3, and MCT4 expression in the retinal pigment epithelium and neural retina of the 5A11/basigin-null mouse. Invest Ophthalmol Vis Sci 44:1305–1311.

Philp NJ, Wang D, Yoon H, Hjelmeland LM. 2003b. Polarized expression of monocarboxylate transporters in human retinal pigment epithelium and ARPE-19 cells. Invest Ophthalmol Vis Sci 44:1716–1721.

Poole RC, Halestrap AP. 1993. Transport of lactate and other monocarboxylates across mammalian plasma membranes. Am J Physiol 264:C682–C761.

Pushkarsky T, Zybarth G, Dubrovsky L, Yurchenko V, Tang H, Guo H, Toole B, Sherry B, Bukrinsky M. 2001. CD147 facilitates HIV-1 infection by interacting with virus-associated cyclophilin A. Proc Natl Acad Sci USA 98:6360–6365.

Saxena DK, Oh-Oka T, Kadomatsu K, Muramatsu T, Toshimori K. 2002. Behaviour of a sperm surface transmembrane glycoprotein basigin during epididymal maturation and its role in fertilization in mice. Reproduction 123:435–444.

Toyama Y, Maekawa M, Kadomatsu K, Miyauchi T, Muramatsu T, Yuasa S. 1999. Histological characterization of defective spermatogenesis in mice lacking the basigin gene. Anat Histol Embryol 28:205–213.

Wilson MC, Meredith D, Halestrap AP. 2002. Fluorescence resonance energy transfer studies on the interaction between the lactate transporter MCT1 and CD147 provide information on the topology and stoichiometry of the complex in situ. J Biol Chem 277:3666–3672.

Wilson MC, Meredith D, Manning Fox JE, Manoharan C, Davies AJ, Halestrap AP. 2005. Basigin (CD147) is the target for organomercurial inhibition of monocarboxylate transporter isoforms 1 and 4: the ancillary protein for the insensitive MCT2 is embigin (gp70). J Biol Chem 280:27213–27221.

Yuasa J, Toyama Y, Miyauchi T, Maekawa M, Yuasa S, Ito H. 2001. Specific localization of the basigin protein in human testes from normal adults, normal juveniles, and patients with azoospermia. Andrologia 33:293–299.

Zucker S, Hymowitz M, Rollo EE, Mann R, Conner CE, Cao J, Foda HD, Tompkins DC, Toole BP. 2001. Tumorigenic potential of extracellular matrix metalloproteinase inducer. Am J Pathol 158:1921–1928.